

Lithospheric Control on Late Cenozoic Magmatism at the Boundary of the Tuva–Mongolian Massif, Khubsugul Area, Northern Mongolia

E. I. Demonerova, A. V. Ivanov, S. V. Rasskazov, M. E. Markova,
T. A. Yasnygina, and Yu. M. Malykh

Institute of the Earth's Crust, Siberian Division, Russian Academy of Sciences, ul. Lermontova 128, Irkutsk, 664033 Russia
e-mail: dem@crust.irk.ru

Received October 1, 2005

Abstract—Late Cenozoic lavas from the western wall of the Khubsugul rift trough were erupted within the Tuva–Mongolian Massif with a pre-Vendian basement, and the lavas in the eastern wall of the trough were erupted within Early Caledonian terranes. The composition of the lavas was determined to vary across the strike of the boundary of the Tuva–Mongolian Massif. The western wall of the trough is dominated by hawaiites and contains subordinate volumes of basanites and much lower amounts of olivine tholeiites and basaltic trachyandesites. The eastern wall contains, in addition to hawaiites, widespread olivine tholeiites and basaltic andesites with subordinate amounts of basaltic trachyandesites. The boundary zone contains practically all rock types (except basaltic andesites) in roughly equal proportions. The trace-element simulations of the partial melting processes demonstrate that the basaltic magmas were produced mainly by 0.5–5% partial melting of garnet lherzolite, with the probable mixing with partial melts derived from spinel lherzolite. The main factor controlling the compositional variations of the lavas was likely the variable depths of their derivation due to variations in the lithosphere thickness at the boundary of the Tuva–Mongolian Massif. Based on the assumption that the source of the magmas was relatively homogeneous and on the results of simulations with the use of experimental data on peridotite melting, we concluded that the asthenospheric sources of the basaltic magmas occurred at depths of 75 ± 10 km (24.6 ± 3.2 kbar) beneath the Tuva–Mongolian Massif and at 60 ± 12 km (20.1 ± 3.8 kbar) beneath the Early Caledonian terranes.

DOI: 10.1134/S0869591107010055

INTRODUCTION

Lateral variations in the trace-element and isotopic characteristics of continental basaltic rocks and deep nodules in them are often thought to be related to the involvement of lithospheric domains of various ages in the melting processes (Menzies, 1989; Leat et al., 1991; Peccerillo and Panza, 1999; Lenoix et al., 2000; Miller et al., 2000; Downes et al., 2003). The southwestern part of the Baikal rift system includes the Tuva–Mongolian Massif, which has a pre-Vendian age and is overlain by a Vendian–Cambrian cover (Il'in, 1971). Its southern boundary is inherited by the Tunka rift valley (Vasil'ev et al., 1997). This boundary can be localized based on changes in the composition of mantle xenoliths (Rasskazov et al., 2000) and isotopic variations in the Late Cenozoic erupted basaltic rocks across the boundary of the Riphean Tuva–Mongolian Massif (Rasskazov et al., 2002a, 2002b). No significant melt volumes can be produced in relatively cold mantle lithosphere with predominantly conductive heat transfer, and the sublithospheric mantle seems to provide more favorable conditions for melting. The drastic variations in the lithosphere thickness at the boundaries of blocks of various ages can facilitate local convective

heat redistribution (King and Anderson, 1998). Domains with low lithospheric thicknesses can serve as traps for hot deep-seated material (Thompson and Gibson, 1991). Hence, the following two mechanisms of magmatic processes can operate in the initially heterogeneous lithosphere: (i) immediate involvement of material of variable age and composition in the melting processes and (ii) the derivation of sublithospheric magmas at various depths. The former scenario obviously implies that the isotopic and trace-element ratios of the magmatic rocks should vary across the boundaries of blocks of various ages, whereas the latter scenario suggests that the rocks should display variations in their major-element compositions, which depend on the P – T conditions of magma derivation.

The Khubsugul area belongs to the southwestern part of the Baikal rift system. The Khubsugul rift valley traces the junction of the Tuva–Mongolian Massif and the Dzhida, Khamar-Daban, and Tunka terranes, which were accreted to the massif in the Early Paleozoic (Belichenko et al., 2003; Kuzmichev, 2004). The problem of the lithospheric control of the magma-generating processes at this structural boundary is considered in this publication on the basis of geochemical and pet-

rological data obtained on the Late Cenozoic volcanic rocks.

FACTUAL MATERIAL

The major- and trace-element characteristics of the Late Cenozoic volcanic rocks are analyzed in correlation with their spatial position relative to the walls of the Khubsugul trough corresponding to different structures of the ancient basement. The volcanic rocks in the western wall are located within the Tuva–Mongolian Massif, and the rocks in the eastern wall occur in the western margin of Caledonian terranes. A transitional zone was distinguished in the northern part of the Khubsugul trough, near the western margin of the Tunka (Il'chi) Caledonian zone that is thrust over the basement of the Tuva–Mongolian Massif (Zorin et al., 1993; Belichenko et al., 2003).

Cenozoic lava piles in the western wall of the Khubsugul trough are strongly eroded and now remain only in the form of separated relict fragments at mountaintops and flow fragments in ancient valleys. The lava piles in the eastern wall of the trough consist of a number of large and well preserved lava flows.

The radiogenic ages of Late Cenozoic lavas from the Khubsugul area were published elsewhere (Amirkhanov et al., 1989; Ivanenko et al., 1989; Yarmolyuk et al., 2003; Rasskazov et al., 2003), but it is quite difficult to use them for the purposes of studying the magmatic processes because of the usual absence of information on the coordinates of the sampling sites and the compositions of the dated rocks. Nevertheless, the Early and Late Miocene magmatic episodes are distinguished fairly reliably, and their products were found in both walls of the trough. Relics of the Early and Late Miocene lavas are contained in roughly equal amounts in the western wall of the trough. Information on the proportions of the early and late lava generations in the eastern wall of the Khubsugul trough is still insufficient, and preliminary estimates indicate that the Late Miocene rocks are predominant.

Data on the compositional variations in the Khubsugul lavas were published in (Kiselev et al., 1979; Rasskazov, 1990; Yarmolyuk et al., 2003). This paper significantly appends preexisting data with newly obtained materials on 227 samples, which were collected during fieldwork in 2001 and 2002. The samples were taken from the vertical sections of the Khubsugul volcanic rocks (Fig. 1). Major elements were determined by conventional chemical techniques in 115 representative samples at the Analytical Center of the Institute of the Earth's Crust, Siberian Division, Russian Academy of Sciences, in Irkutsk, and 76 samples were analyzed for many trace elements by ICP-MS on a PlasmaQuad II+ mass spectrometer at the Baikal Analytical Center for Collective Use (Chebykin et al., 2004). Samples were prepared at the Laboratory of Isotopic Research and Geochronology of the Institute of the

Earth's Crust, Siberian Division, Russian Academy of Sciences. The analytical errors were no higher than 5% for most elements. The analytical techniques and procedures were described in detail in (Yasnygina et al., 2003). Selected analyses are presented in the table. With regard for the high representativeness of our sample collection, we used only our own analytical data in order to eliminate potential interlaboratory discrepancies.

ROCK SYSTEMATICS

Most volcanic rocks from the Khubsugul area belong to the moderately alkaline series (Fig. 2a). According to (*Classification of Magmatic...*, 1997), most of their data points plot within the field of trachybasalt and, to a lesser extent, basalt, basanite, basaltic andesite, and basaltic trachyandesite in the $(\text{Na}_2\text{O} + \text{K}_2\text{O})\text{-SiO}_2$ diagram (Fig. 2a). According to the variations in the Na_2O , K_2O , and SiO_2 concentrations and the contents of CIPW normative minerals (*Magmatic Rocks...*, 1985; *Classification of Magmatic...*, 1997; Le Bas and Streckeisen, 1991), the rocks are classified into five major groups: basanites, hawaiites, olivine tholeiites, basaltic andesites, and basaltic trachyandesites (Fig. 2b).

Basanites are rocks most strongly undersaturated in silica and containing 8–20% normative nepheline. *Hawaiites* are a sodic variety of trachybasalts with normative nepheline (from 0 to 8%). *Olivine tholeiites* are a variety of basalts with normative olivine and hypersthene (from 0 to 15%). *Basaltic andesites* are rocks of normal alkalinity and with >52 wt % SiO_2 and 15–25% normative hypersthene. *Basaltic trachyandesites* are rocks that plot within the field of moderate alkalinity in a $(\text{Na}_2\text{O} + \text{K}_2\text{O})\text{-SiO}_2$ diagram. They are represented by three holocrystalline samples with $100 \times \text{An}/(\text{An} + \text{Ab}) < 35\%$, which were taken from lenses of essexite rocks up to 10 cm thick in a flow of olivine tholeiite (sample MN-127). *Essexites* (table, sample MN-130) are dominated by large (up to 1.5 cm) variably oriented crystals of plagioclase and pyroxene and flat tabular crystals of an ore mineral (provisionally identified as ilmenite). Rocks with similar petrographic characteristics and chemical composition are widespread in the nearby territory of the Eastern Sayan Range (Rasskazov, 1993). In contrast to typical essexites, our rocks contain no feldspathoids. The other two samples of the basaltic trachyandesites are mugearite (table, samples MN-269, MN-24).

SPATIAL VARIATIONS AND CHEMICAL COMPOSITION OF THE LAVAS

Figure 3 presents histograms for the distribution of rocks of various types in both walls of the Khubsugul trough and in its northern part. The pervasively predominant rock type is hawaiite. In the eastern wall, olivine tholeiites are the second most widely spread rock type, and basaltic andesites are the third one. Our ana-

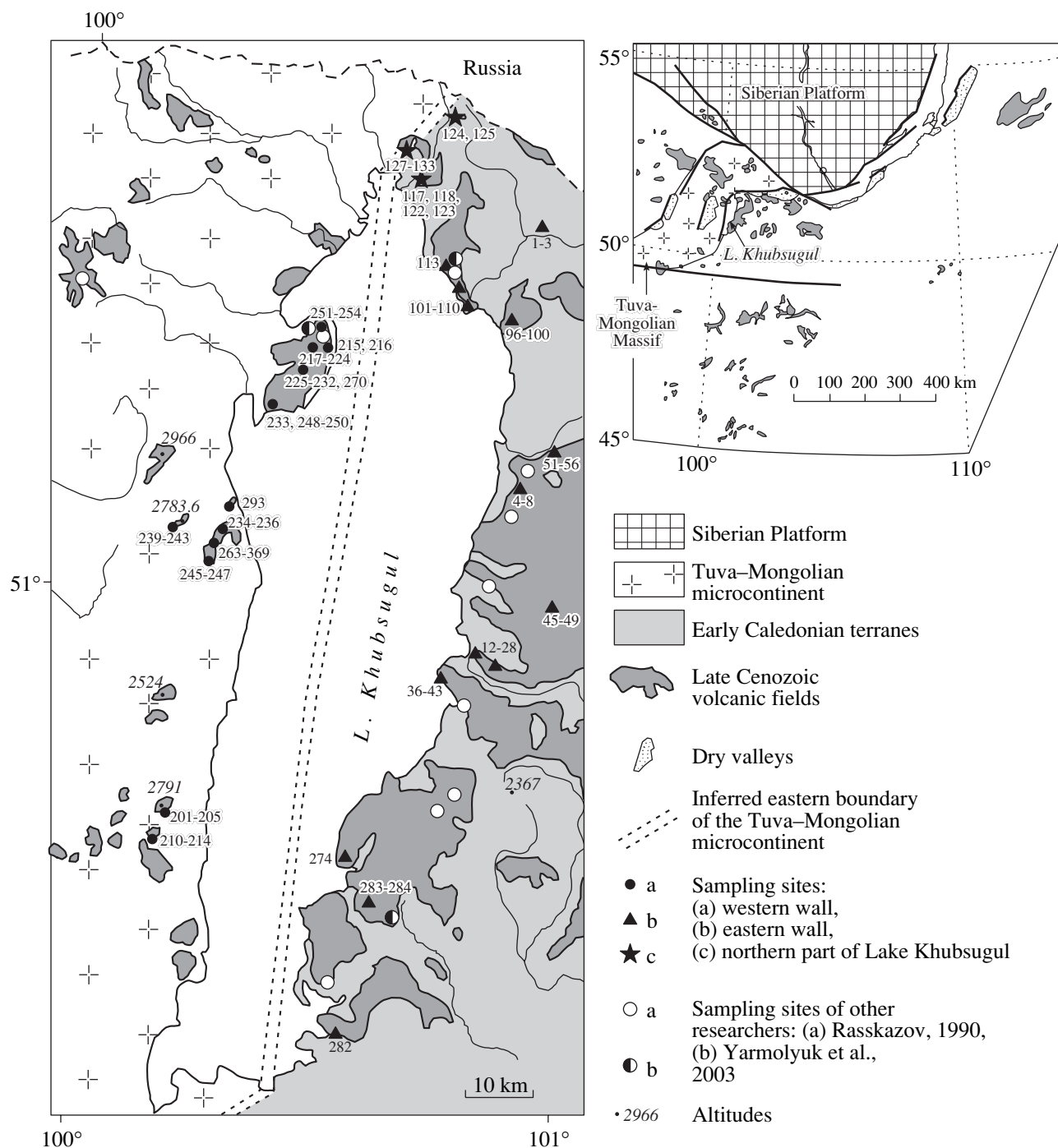


Fig. 1. Schematic map of Late Cenozoic volcanic rocks in the Khubsugul area and their sampling sites.

lyzed samples included no basanites. These rocks were quite often found in the western wall, whereas basaltic andesites were not found in this wall at all. Olivine tholeiites were found only in Dolon-Ula Peninsula. The spatial distribution of the basaltic andesites and olivine tholeiites is consistent with earlier data in (Rasskazov, 1990; Yarmolyuk et al., 2003). The northern part of the trough contains the same rock types as its western wall

and, in contrast to the latter, additionally bears olivine tholeiitic lavas with essexite lenses.

The spatial variations in the petrographic rock types are reflected in the major- and trace-element compositions of the rocks. For example, due to the presence of basaltic andesites and more abundant olivine tholeiites, the lavas of the eastern wall of the Khubsugul trough

Concentrations of major oxides (wt %), normative minerals (wt %), and trace elements (ppm) and calculated pressures (kbar) for representative basalt samples from the Khubsugul area

Component	Western wall of Lake Khubsugul							
	Mount Urun-Dush-Ula		Mongolyn-Yast-Gol River		Dolon-Ula Peninsula			
	MN-202*	MN-205	MN-211	MN-214	MN-215	MN-216	MN-219	MN-224
	50°51.10' 100°10.40'**	50°51.20' 100°10.20'	50°48.40' 100°08.40'	50°48.40' 100°09.20'	51°25.50' 100°27.35'	51°25.50' 100°27.30'	51°25.50' 100°26.60'	51°25.40' 100°26.35'
	H***	H	H	H	H	B	H	H
SiO ₂	47.24	46.91	46.13	47.21	46.5	46.23	47.21	46.62
TiO ₂	2.52	2.41	2.10	2.28	2.52	2.25	1.90	2.00
Al ₂ O ₃	15.95	16.15	15.5	15.45	15.45	14.8	15.9	15.67
Fe ₂ O ₃	2.08	2.01	1.55	2.87	4.55	2.36	2.68	1.89
FeO	9.40	8.91	9.60	8.44	7.02	8.48	7.76	8.13
MnO	0.14	0.14	0.14	0.13	0.14	0.15	0.15	0.14
MgO	7.00	7.85	9.01	8.06	6.27	8.48	8.22	8.08
CaO	7.03	7.83	7.89	8.14	7.28	8.48	7.75	8.51
Na ₂ O	3.87	4.13	3.35	3.17	4.20	4.00	3.82	3.49
K ₂ O	1.82	1.78	1.63	1.60	1.54	2.10	1.50	2.04
P ₂ O ₅	0.78	0.69	0.61	0.58	0.51	0.67	0.61	0.68
H ₂ O ⁻	0.67	0.43	0.48	0.73	0.15	0.32	0.4	0.4
H ₂ O ⁺	1.55	1.26	2.45	1.77	0.58	1.36	1.88	1.97
Total	100.05	100.5	100.44	100.43	96.71	99.68	99.78	99.62
Ne	2.51	6.85	3.53	0.55	4.6	9.51	3.63	5.38
Hy	0	0	0	0	0	0	0	0
An, %	42.39	47.42	50.49	47.32	40.95	49.91	45.99	51.81
P, kbar	25.1	25.3	26.2	24.6	25.1	25.7	22.6	22.9
Sc	17.2	21.5	18.5	19.0	18.4	17.2	18.0	16.5
Rb	16.8	23.5	26.4	29.3	17.8	21.0	20.5	17.1
Sr	703	794	524	730	755	882	867	781
Y	20.1	23.2	24.4	22.8	21.8	20.9	22.9	21.1
Zr	152	185	180	186	185	192	205	184
Nb	33.3	40.2	32.5	40.5	39.2	46.2	50.7	44.9
Sn	1.59	1.69	2.24	1.69	1.84	1.95	1.82	1.78
Cs	0.534	0.42	0.10	0.44	0.26	0.16	0.26	0.26
Ba	259	322	381	447	289	350	359	334
La	22.3	27.3	21.3	25.9	26.1	29.8	31.0	28.9
Ce	46.7	56.9	46.4	55.1	54.4	61.7	64.8	59.7
Pr	5.73	6.93	5.90	7.02	6.65	7.69	8.13	7.41
Nd	23.7	28.8	25.9	29.5	28.1	32.1	34.5	30.7
Sm	5.55	6.62	6.72	6.90	6.48	6.93	7.46	7.04
Eu	1.82	1.98	2.10	2.24	1.97	2.26	2.41	2.23
Tb	0.735	0.859	0.884	0.905	0.860	0.888	0.953	0.874
Gd	4.97	5.80	6.00	6.81	5.81	6.59	7.48	7.02
Dy	3.86	4.34	4.55	4.68	4.28	4.50	4.88	4.58
Ho	0.682	0.750	0.783	0.822	0.749	0.734	0.846	0.800
Er	1.78	2.14	2.25	1.97	1.96	1.89	2.06	2.03
Yb	1.43	1.66	1.85	1.59	1.38	1.40	1.49	1.50
Lu	0.199	0.242	0.233	0.193	0.207	0.175	0.223	0.199
Hf	3.16	3.72	4.40	4.19	3.71	4.18	4.35	4.07
Ta	1.83	2.18	1.92	2.05	2.30	2.67	2.93	2.64
Pb	4.18	3.28	5.98	2.75	2.71	2.71	3.34	2.99
Th	2.24	2.82	2.83	2.44	2.70	3.12	3.04	2.97
U	0.651	0.786	1.121	0.664	0.851	0.896	0.897	0.964

Table (Contd.)

Component	Western wall of Lake Khubsugul							
	Dolon-Ula Peninsula					Uliin-Gol River		
	MN-227	MN-229	MN-232	MN-253	MN-270	MN-236	MN-239	MN-245
	51°24.05' 100°25.50'	51°23.50' 100°25.30'	51°20.40' 100°24.20'	51°26.00' 100°24.10'	51°23.40' 100°25.55'	51°10.35' 100°15.00'	51°10.30' 100°09.20'	51°08.40' 100°13.45'
OT	H	H	B	H	H	H	H	
SiO ₂	49.41	48.93	48.93	45.78	46.21	48.7	46.13	47.43
TiO ₂	2.11	2.38	2.32	1.78	2.48	2.32	2.33	2.10
Al ₂ O ₃	15.45	16.25	16.1	15.67	15.3	15.9	15.9	16.3
Fe ₂ O ₃	2.55	2.93	5.18	2.19	3.27	4.43	2.47	2.40
FeO	7.24	7.79	7.65	9.20	7.56	6.28	8.56	8.45
MnO	0.13	0.12	0.09	0.12	0.14	0.14	0.12	0.12
MgO	7.00	6.47	6.58	8.07	8.11	6.54	7.09	7.45
CaO	7.19	7.93	7.93	7.60	8.26	7.77	7.24	6.81
Na ₂ O	3.84	4.07	4.04	3.96	3.32	4.22	3.80	4.11
K ₂ O	1.61	1.45	1.73	2.18	2.12	1.85	1.84	1.65
P ₂ O ₅	0.47	0.60	0.62	0.94	0.83	0.60	1.01	0.65
H ₂ O ⁻	1.27	0.28	0.18	2.02	0.52	0.23	0.50	0.45
H ₂ O ⁺	1.91	0.54	0.68	1.60	2.16	0.82	2.92	2.02
Total	100.18	99.74	102.03	101.11	100.28	99.8	99.91	99.94
<i>Ne</i>	0	1.79	3.49	8.13	4.24	4.27	2.87	3.46
<i>Hy</i>	2.11	0	0	0	0	0	0	0
<i>An</i> , %	38.30	41.16	42.72	50.07	50.12	40.55	43.6	42.71
<i>P</i> , kbar	16.7	21.2	26.3	27.4	25.3	21.3	25.4	23.1
Sc	16.8	17.2	17.9	14.9	n.a.	18.9	15.4	16.8
Rb	15.9	19.9	19.7	24.5	29.4	16.4	23.7	18.9
Sr	765	864	845	1020	1069	690	1030	718
Y	19.4	21.7	21.6	23.0	26.2	22.1	23.5	22.8
Zr	164	191	196	248	250	191	213	181
Nb	38.3	43.6	45.1	63.6	64.1	39.3	55.5	39.0
Sn	1.67	1.87	1.79	2.16	2.49	1.81	2.00	1.73
Cs	0.29	0.30	0.29	0.37	0.53	0.14	0.47	0.51
Ba	294	292	388	358	551	313	319	274
La	24.5	27.9	29.5	36.6	40.4	26.6	39.0	25.1
Ce	52.4	58.1	62.3	75.9	79.6	55.8	80.9	53.0
Pr	6.58	6.93	7.66	9.27	9.05	6.83	9.76	6.61
Nd	27.5	29.7	31.3	37.7	41.0	29.1	40.4	28.2
Sm	6.39	6.51	7.05	8.26	9.18	6.39	8.99	6.33
Eu	1.97	2.19	2.27	2.62	3.19	2.09	2.71	2.08
Tb	0.781	0.896	0.916	1.058	1.087	0.853	1.025	1.057
Gd	6.02	5.81	6.77	7.23	8.77	5.73	7.37	5.65
Dy	4.14	4.20	4.70	5.01	5.81	4.26	4.75	4.49
Ho	0.744	0.708	0.826	0.827	1.038	0.718	0.752	0.784
Er	1.69	1.77	2.07	1.98	2.62	2.01	2.04	2.08
Yb	1.32	1.33	1.58	1.29	1.70	1.51	1.41	1.58
Lu	0.192	0.189	0.210	0.178	0.262	0.221	0.191	0.221
Hf	3.59	3.99	4.04	5.19	5.80	4.11	4.35	3.65
Ta	2.17	2.47	2.45	3.76	3.90	2.24	2.93	2.25
Pb	2.71	2.77	2.96	3.31	3.46	3.15	3.62	2.87
Th	2.54	2.68	2.69	3.89	3.87	2.66	3.44	2.80
U	0.726	0.854	0.807	1.195	1.156	0.768	0.976	0.786

Table (Contd.)

Component	Western wall of Lake Khubsugul		Eastern wall of Lake Khubsugul					
	Uliin-Gol River			Sevsulin-Gol River				Ovotyn-Daba Pass
	MN-269	MN-293	MN-2	MN-4	MN-5	MN-6	MN-8	MN-16
	51°09.35' 100°14.30'	51°12.40' 100°16.20'	51°35.40' 100°48.30'	51°10.10' 100°45.91'	51°10.10' 100°45.91'	51°10.10' 100°45.91'	51°10.10' 100°45.91'	51°04.50' 100°42.52'
	Mg	H	OT	H	OT	H	H	OT
SiO ₂	50.58	47.58	47.84	47.38	49.5	47.43	46.67	51.49
TiO ₂	1.98	2.29	2.28	2.18	2.06	2.06	2.63	1.98
Al ₂ O ₃	15.18	15.16	14.1	15.55	15.85	15.45	15.15	16.0
Fe ₂ O ₃	1.51	2.8	2.26	2.76	1.93	2.71	1.88	3.23
FeO	8.92	8.03	8.69	7.68	7.60	6.85	9.12	5.48
MnO	0.15	0.15	0.15	0.12	0.13	0.14	0.15	0.16
MgO	6.25	7.81	9.99	6.65	7.22	8.78	7.17	5.14
CaO	6.99	8.57	7.69	7.00	7.84	7.76	7.77	8.26
Na ₂ O	4.33	3.29	3.15	3.6	3.55	3.35	3.93	3.70
K ₂ O	1.74	1.86	1.24	2.26	1.56	1.55	2.08	0.89
P ₂ O ₅	0.62	0.62	0.61	1.18	0.69	0.78	0.87	0.34
H ₂ O ⁻	0.20	0.23	0.17	0.33	0.28	0.28	0.13	0.28
H ₂ O ⁺	1.66	1.16	2.17	3.43	1.52	3.29	2.92	3.03
Total	100.11	99.55	100.34	100.12	99.73	100.15	100.47	99.98
<i>Ne</i>	0.35	2.21	0	0.58	0	0.02	5.56	0
<i>Hy</i>	0	0	5.12	0	6.12	0	0	16.39
<i>An, %</i>	31.88	46.96	43.69	39.96	43.05	44.32	42.96	43.83
<i>P, kbar</i>	17.3	23.2	22.3	21.7	16.8	19.5	25.0	10.6
Sc	21.0	19.5	11.8	8.4	n.a.	16.6	10.4	13.1
Rb	18.6	16.7	15.7	26.4	22.7	16.5	27.9	33.7
Sr	710	805	901	1121	1088	919	1213	739
Y	22.8	22.0	18.4	19.5	26.2	21.4	20.7	16.7
Zr	174	211	174	242	224	218	236	101
Nb	47.0	45.4	35.3	66.6	46.6	47.7	62.4	32.0
Sn	1.49	1.63	1.49	2.49	2.02	1.65	1.79	1.02
Cs	0.40	0.07	0.18	0.22	0.19	0.31	0.39	1.68
Ba	281	618	334	419	463	435	371	761
La	26.4	28.2	23.8	51.3	35.3	34.6	35.5	19.0
Ce	48.3	59.4	51.4	102.7	71.5	70.6	73.8	34.6
Pr	6.50	6.95	6.35	12.17	7.78	8.20	8.76	3.94
Nd	29.7	30.4	29.3	52.3	36.3	34.6	38.2	18.2
Sm	5.98	6.62	6.62	10.56	8.08	7.17	8.73	4.53
Eu	2.07	2.11	2.21	3.27	2.62	2.29	2.71	1.80
Tb	6.283	0.829	0.815	1.128	1.075	0.875	0.992	0.660
Gd	0.83	6.14	5.51	7.83	6.75	5.76	7.02	4.00
Dy	4.22	4.34	4.19	5.07	5.43	4.63	4.92	3.49
Ho	0.787	0.817	0.645	0.719	1.166	0.786	0.762	0.610
Er	2.00	1.99	1.88	1.67	2.63	2.06	1.87	1.55
Yb	1.75	1.47	1.23	1.00	1.95	1.45	1.27	1.23
Lu	0.234	0.201	0.177	0.136	0.312	0.210	0.170	0.179
Hf	4.53	4.63	3.90	4.82	4.77	4.22	4.98	2.52
Ta	2.40	2.39	2.02	3.19	2.71	2.34	3.41	1.44
Pb	3.35	1.50	2.00	2.89	4.01	3.10	2.96	2.64
Th	2.39	2.19	2.14	3.47	2.77	2.89	3.28	1.99
U	0.830	0.833	0.674	1.092	0.672	0.948	1.107	0.551

Table (Contd.)

Component	Eastern wall of Lake Khubsugul							
	Ovotyn-Daba Pass			Borsogiin-Daba Pass			Ikh-Noen-Gol River	
	MN-18	MN-22	MN-24	MN-36	MN-42	MN-43	MN-45	MN-49
	51°01.72' 100°46.02'	51°01.72' 100°46.02'	51°01.72' 100°46.02'	51°00.39' 100°42.27'	51°00.55' 100°42.23'	51°00.55' 100°42.23'	51°13.53' 100°50.35'	51°13.53' 100°50.35'
	OT	H	Mg	B	B	H	OT	H
SiO ₂	50.4	46.7	49.68	52.36	52.29	47.24	47.71	48.52
TiO ₂	2.48	2.38	2.05	2.10	1.88	2.80	1.96	2.10
Al ₂ O ₃	15.55	15.1	15.55	15.25	17.33	15.55	16.8	17.2
Fe ₂ O ₃	1.80	2.17	3.34	2.13	5.54	6.22	3.00	4.61
FeO	9.70	9.23	6.39	8.00	4.19	6.73	6.23	5.26
MnO	0.27	0.17	0.07	0.14	0.11	0.16	0.13	0.14
MgO	6.58	8.26	5.64	6.98	5.31	6.76	6.83	5.28
CaO	7.47	8.67	6.56	7.77	7.42	7.17	7.85	7.98
Na ₂ O	3.76	3.56	4.16	3.57	3.50	4.21	3.00	3.42
K ₂ O	1.30	1.62	2.63	1.14	1.19	1.84	2.26	2.40
P ₂ O ₅	0.51	0.61	1.16	0.42	0.38	0.74	0.79	0.95
H ₂ O ⁻	0	0.12	0.17	0.05	0.13	0.15	0.84	0.91
H ₂ O ⁺	0.65	1.86	3.09	0.61	0.74	0.70	2.86	1.72
Total	100.47	100.45	100.49	100.52	100.01	100.27	100.26	100.49
<i>Ne</i>	0	4.81	1.04	0	0	5.11	0	0.29
<i>Hy</i>	9.36	0	0	20.4	21.18	0	2.52	0
<i>An, %</i>	40.56	48.86	32.42	42.39	48.66	40.76	47.36	40.18
<i>P, kbar</i>	20.8	26.3	16.6	14.1	12.9	28.2	18.6	19.6
<i>Sc</i>	13.9	n.a.	18.0	13.5	15.9	n.a.	18.4	20.3
<i>Rb</i>	20.0	22.4	36.4	20.7	16.2	30.8	27.9	28.0
<i>Sr</i>	580	845	1312	532	565	995	996	1028
<i>Y</i>	20.2	24.1	19.6	18.3	16.7	26.1	23.0	25.7
<i>Zr</i>	178	230	329	159	158	300	211	302
<i>Nb</i>	30.4	55.6	78.5	24.9	21.3	64.2	40.1	48.5
<i>Sn</i>	1.43	2.34	2.96	1.40	1.39	2.79	1.68	1.59
<i>Cs</i>	0.10	0.22	0.43	1.07	0.24	0.42	0.43	0.32
<i>Ba</i>	362	382	502	1412	393	431	474	516
<i>La</i>	19.6	30.9	45.0	16.9	16.9	37.8	32.3	36.3
<i>Ce</i>	43.8	62.1	95.9	37.3	37.0	82.4	66.4	74.3
<i>Pr</i>	5.67	7.40	11.27	4.91	4.73	9.83	7.82	8.42
<i>Nd</i>	27.6	32.8	50.2	23.0	22.3	46.7	34.3	37.4
<i>Sm</i>	6.97	7.65	10.44	6.04	5.78	10.50	6.74	7.39
<i>Eu</i>	2.32	2.42	3.46	2.13	1.90	3.32	2.32	2.51
<i>Tb</i>	0.905	0.955	1.106	0.737	0.702	1.251	0.875	0.961
<i>Gd</i>	6.09	7.42	8.35	5.02	4.64	8.50	5.96	6.66
<i>Dy</i>	4.64	5.76	4.71	3.89	3.52	5.97	4.25	4.87
<i>Ho</i>	0.760	0.937	0.676	0.684	0.599	1.025	0.773	0.851
<i>Er</i>	1.85	2.39	1.60	1.80	1.50	2.44	2.07	2.18
<i>Yb</i>	1.31	1.67	0.91	1.34	1.16	1.81	1.60	1.73
<i>Lu</i>	0.189	0.295	0.117	0.182	0.177	0.224	0.219	0.248
<i>Hf</i>	4.19	4.62	7.14	3.66	3.60	6.52	4.29	6.24
<i>Ta</i>	1.62	3.23	4.79	1.32	1.11	3.70	2.26	2.72
<i>Pb</i>	1.80	3.72	4.11	2.38	4.42	3.10	3.16	3.39
<i>Th</i>	1.68	3.14	4.41	1.53	1.35	3.47	3.11	3.43
<i>U</i>	0.336	0.895	1.333	0.380	0.441	1.033	0.891	0.984

Table (Contd.)

Component	Eastern wall of Lake Khubsugul							
	Settlement of Turtu			Khankh-Gol River			Southeastern part of Lake Khubsugul	
	MN-103	MN-105	MN-111	MN-96	MN-98	MN-99	MN-274	MN-282
	51°31.20' 100°38.58'	51°31.35' 100°39.00'	51°31.40' 100°39.10'	51°27.37' 100°41.97'	51°27.37' 100°41.97'	51°27.37' 100°41.97'	50°32.40' 100°30.01'	50°37.15' 100°31.40'
	H	OT	OT	H	H	H	H	H
SiO ₂	49.65	49.18	49.43	48.77	46.76	46.59	49.48	49.81
TiO ₂	2.39	2.36	2.42	2.10	2.46	2.40	2.43	2.44
Al ₂ O ₃	15.55	15.35	15.65	15.95	14.3	14.3	15.42	15.5
Fe ₂ O ₃	2.70	8.90	3.36	1.90	2.96	3.67	2.68	5.71
FeO	6.98	3.10	7.14	8.53	8.01	7.93	8.68	5.28
MnO	0.12	0.15	0.14	0.13	0.12	0.13	0.14	0.12
MgO	6.55	6.15	7.15	6.45	8.81	8.76	7.03	6.54
CaO	7.85	7.88	7.82	7.90	8.5	8.20	8.01	7.89
Na ₂ O	4.12	3.47	3.70	4.21	3	3.14	3.70	3.84
K ₂ O	2.58	1.83	1.72	1.40	1.9	1.99	1.60	1.77
P ₂ O ₅	0.70	0.72	0.63	0.55	0.62	0.63	0.50	0.56
H ₂ O ⁻	0.02	0.23	0.18	0.06	0.3	0.28	0.03	0.03
H ₂ O ⁺	0.61	1.10	1.15	1.72	2.67	2.44	0.60	0.91
Total	99.82	100.42	100.49	99.67	100.41	100.46	100.3	100.4
<i>Ne</i>	4.99	0	0	2.64	2.67	3.01	0.26	0.4
<i>Hy</i>	0	4.71	0.17	0	0	0	0	0
<i>An</i> , %	38.79	41.6	40.18	39.89	47.57	47.36	40.23	38.45
<i>P</i> , kbar	18.0	22.4	19.8	20.4	24.3	26.0	21.9	20.0
<i>Sc</i>	n.a.	n.a.	n.a.	24.1	13.5	12.3	19.8	17.8
<i>Rb</i>	51.3	40.7	21.2	18.6	22.3	19.4	23.3	21.9
<i>Sr</i>	1062	959	1018	714	911	821	620	623
<i>Y</i>	25.8	27.2	25.6	19.7	18.5	18.5	24.9	23.0
<i>Zr</i>	247	228	239	534	195	194	182	197
<i>Nb</i>	57.9	42.4	44.8	27.7	48.2	48.2	35.3	40.9
<i>Sn</i>	2.73	2.56	2.43	1.81	2.57	2.17	2.11	1.94
<i>Cs</i>	1.20	1.93	0.30	0.18	0.333	0.18	0.19	0.34
<i>Ba</i>	562	493	440	281	363	367	382	401
<i>La</i>	40.4	36.8	33.3	20.1	27.9	27.8	18.6	22.2
<i>Ce</i>	80.3	74.8	69.4	44.3	58.7	57.8	41.3	46.6
<i>Pr</i>	9.35	8.78	8.58	5.37	6.95	6.92	5.93	6.06
<i>Nd</i>	40.8	38.4	41.0	25.7	30.4	30.7	26.5	28.1
<i>Sm</i>	9.50	8.46	9.18	6.00	6.80	6.55	6.58	7.01
<i>Eu</i>	2.62	2.69	2.78	2.08	2.18	2.20	2.28	2.30
<i>Tb</i>	1.026	1.110	0.958	0.734	0.840	0.897	0.877	0.844
<i>Gd</i>	7.03	8.12	8.02	5.46	5.50	5.60	6.16	6.02
<i>Dy</i>	5.85	6.02	5.99	3.69	4.30	4.18	4.51	4.21
<i>Ho</i>	1.033	1.128	1.009	0.659	0.684	0.747	0.804	0.831
<i>Er</i>	2.34	2.48	2.53	1.78	1.68	1.86	1.90	2.08
<i>Yb</i>	1.68	1.91	1.59	1.40	1.296	1.31	1.51	1.44
<i>Lu</i>	0.222	0.304	0.252	0.216	0.178	0.160	0.174	0.165
<i>Hf</i>	6.26	4.74	5.46	12.71	4.11	4.04	4.24	4.71
<i>Ta</i>	3.69	2.41	2.55	1.74	2.55	2.48	1.69	2.16
<i>Pb</i>	6.23	6.40	4.21	1.89	3.42	2.65	2.03	2.92
<i>Th</i>	5.36	4.89	2.91	2.18	2.59	2.79	1.60	1.99
<i>U</i>	1.28	1.17	0.669	0.821	0.900	0.913	0.478	0.700

Table (Contd.)

Component	Northern part of the depression of Lake Khubsugul						
	North of settlement of Turtu						
	MN-118	MN-123	MN-125	MN-127	MN-130	MN-132	MN-133
	51°36.39' 100°37.30'	51°36.90' 100°35.17'	51°41.25' 100°41.33'	51°38.01' 100°34.54'	51°38.01' 100°34.54'	51°38.01' 100°34.54'	51°38.01' 100°34.54'
	H	B	H	OT	Es	B	OT
SiO ₂	48.8	45.31	46.42	48.53	50.1	45.34	48.21
TiO ₂	2.72	2.31	2.39	2.41	4.31	2.96	2.96
Al ₂ O ₃	14.5	15.75	16.15	14.75	15.15	14.25	14.35
Fe ₂ O ₃	3.81	2.11	2.00	2.35	2.72	2.88	3.85
FeO	7.53	8.91	9.31	9.69	7.83	9.21	8.86
MnO	0.16	0.14	0.08	0.15	0.13	0.15	0.14
MgO	7.44	8.87	8.32	8.31	3.63	8.09	6.23
CaO	8.48	8.10	7.83	7.52	8.14	7.84	6.29
Na ₂ O	3.86	3.72	4.06	3.40	3.86	3.68	3.34
K ₂ O	1.77	1.95	1.62	1.51	2.13	2.76	2.29
P ₂ O ₅	0.55	0.72	0.64	0.55	0.74	0.98	1.04
H ₂ O ⁻	0.07	0.47	0.53	0.17	0.22	0.16	0.47
H ₂ O ⁺	0.64	1.84	1.12	0.76	1.30	2.18	1.84
Total	100.33	100.2	100.47	100.1	100.26	100.48	100.34
Ne	3.47	8.2	6.99	0	0	9.03	0
Hy	0	0	0	2.44	6.13	0	10.46
P, kbar	22.8	27.8	26.9	24.4	19.4	29.8	25.2
Sc	n.a.	11.4	16.0	n.a.	n.a.	n.a.	n.a.
Rb	26.9	15.2	25.0	28.8	29.7	36.8	33.6
Sr	795	575	643	835	793	1309	1257
Y	26.5	14.3	21.4	24.8	24.8	28.0	27.8
Zr	240	129	175	255	278	359	365
Nb	51.7	31.0	36.5	52.0	65.2	87.7	92.4
Sn	2.68	1.13	1.88	2.47	2.16	3.24	3.23
Cs	0.33	0.27	0.72	0.37	0.22	0.78	0.60
Ba	410	279	402	404	498	772	561
La	30.1	18.6	23.6	29.1	36.2	54.1	52.3
Ce	62.6	40.6	50.5	60.0	73.7	109.9	107.4
Pr	7.63	5.04	6.38	6.94	9.32	12.58	12.58
Nd	34.3	20.9	27.4	33.1	40.0	57.8	54.5
Sm	8.73	4.46	6.53	7.72	8.84	11.47	12.20
Eu	2.60	1.47	2.12	2.35	2.85	3.59	3.67
Tb	1.08	0.580	0.868	1.02	1.25	1.43	1.36
Gd	6.84	4.02	5.79	7.21	8.27	9.42	9.98
Dy	6.23	2.85	4.45	5.90	5.65	6.27	5.91
Ho	1.12	0.490	0.743	1.01	1.031	1.09	1.04
Er	2.72	1.21	1.94	2.24	2.44	2.51	2.61
Yb	2.02	0.89	1.35	1.82	1.77	1.53	1.64
Lu	0.292	0.119	0.187	0.231	0.266	0.191	0.255
Hf	5.91	2.74	3.87	5.67	6.90	7.68	8.01
Ta	3.31	1.74	2.04	3.09	3.97	5.28	5.68
Pb	3.35	2.04	2.95	4.03	3.87	4.74	4.38
Th	3.04	1.92	2.47	3.17	3.32	5.33	5.47
U	0.913	0.589	0.677	0.807	0.636	1.622	1.700

Note: Whole set of analyses is available from the author via e-mail: dem@crust.irk.ru.

* Sample no.

** Coordinates of the sampling sites.

*** Rocks: H—hawaiite, OT—olivine tholeiite, B—basalt, BA—basaltic andesite, BTA—basaltic trachyandesite, Mg—mugearite, Es—essxite.

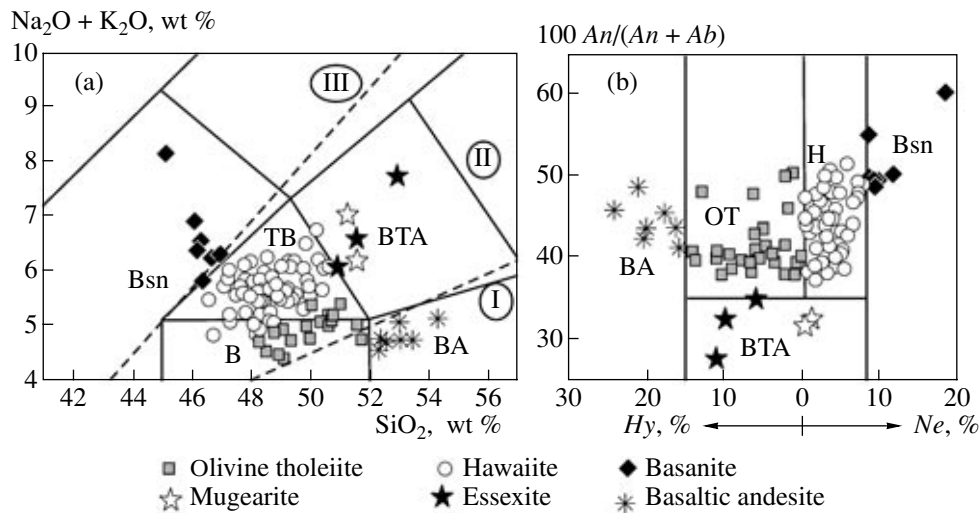


Fig. 2. Classification diagrams: (a) $(\text{Na}_2\text{O} + \text{K}_2\text{O})\text{-SiO}_2$, (b) $100 \text{An}/(\text{An} + \text{Ab})$ vs. Ne-Hy for Late Cenozoic lavas in the Khubsugul area.

(a) Solid lines show the boundaries of compositional fields after (*Classification of Magmatic...*, 1997), dashed lines show the boundaries of rocks of (I) normal, (II) moderately alkaline, and (III) alkaline series (*Magmatic Rocks...*, 1985). The compositions used in the diagram were normalized to 100 wt % anhydrous residue.

(b) In calculating the normative minerals, the FeO and Fe_2O_3 concentrations were determined from the relation $\text{Fe}^{3+} = 0.15 \text{Fe}_{\text{tot}}$ (at. quant.). Rocks: Bsn—basanite, B—basalt, BTA—basaltic trachyandesite, BA—basaltic andesite, TB—trachybasalt, H—hawaiiite, OT—olivine tholeiite.

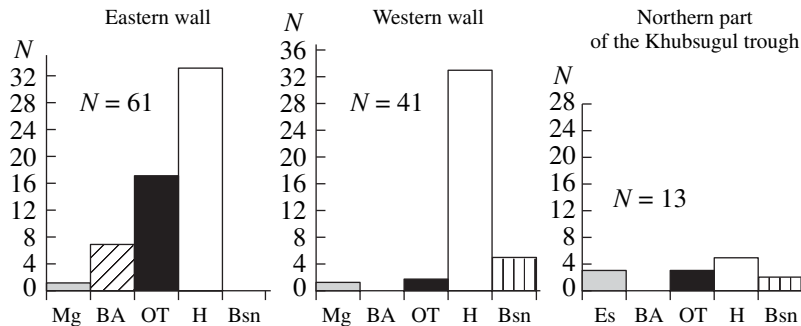


Fig. 3. Histograms for the occurrence frequencies of various rock types in the eastern and western walls of the Khubsugul rift trough and in its northern part. Rocks: Bsn—basanite, H—hawaiiite, OT—olivine tholeiite, BA—basaltic andesite and basaltic trachyandesite, Mg—mugearite, Es—essexite

exhibit broader compositional variations than those of the western-wall lavas.

The SiO_2 concentrations in lavas from the western wall of the Khubsugul trough vary from 45 to 51.8 wt % at $\text{Na}_2\text{O} + \text{K}_2\text{O}$ from 4.7 to 8 wt %. Because of the absence of basanites from the eastern wall and the appearance of basaltic andesites, the variation range of the SiO_2 concentrations shifts toward higher values (from 47.5 to 54.5 wt %), whereas the values of $\text{Na}_2\text{O} + \text{K}_2\text{O}$ shift to lower values (from 4.3 to 7 wt %). The lavas in the northern part of the trough contain 46.3–53 wt % SiO_2 at $\text{Na}_2\text{O} + \text{K}_2\text{O}$ from 4.6 to 7.5 wt %.

The lavas from the western wall are characterized by broad ranges of their P_2O_5 contents, from 0.5 to 1.3 wt %. A similar range of P_2O_5 concentrations (from

0.5 to 1.2 wt %) was determined in the lavas from the northern part of the trough. The P_2O_5 concentrations in the lavas from the eastern wall are from 0.4 to 0.9 wt %. The MgO concentrations in the lavas from both walls and the northern part of the trough range from 2.7 to 11.1 wt %, and the TiO_2 concentrations are 1.5–4.4 wt %. The lowest MgO concentrations and high TiO_2 and P_2O_5 contents occur in essexite lenses from an olivine tholeiitic flow in the transitional zone (table).

The volcanic rocks from the Khubsugul area generally have trace- and minor-element concentrations close to those of average within-plate basalt of oceanic islands (OIB) (Sun and McDonough, 1984) (Fig. 4) but differ from the latter in having Th–U, La–Ce, and Zr–Hf minima in the elemental patterns and relatively low

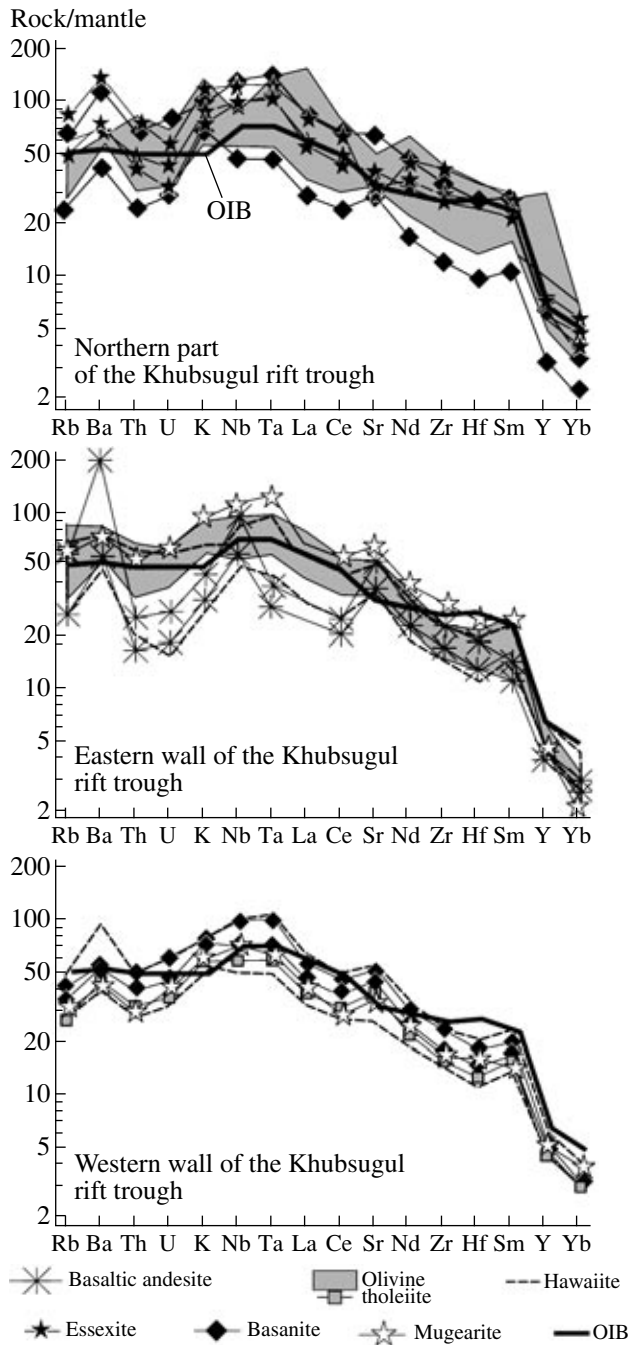


Fig. 4. Undifferentiated mantle-normalized (Sun and McDonough, 1989) incompatible-element patterns for various rock types from the Khubsugul area.

The average trace-element composition of oceanic-island basalts (OIB) is compiled from (Sun and McDonough, 1989).

concentrations of HREE at elevated contents of Ba, Nb, Ta, and Sr. Lavas from the western wall differ from lavas from the eastern wall and the northern part of the trough in displaying narrower ranges of the concentrations of most trace elements because of the absence of basaltic andesites from the former rock group and a

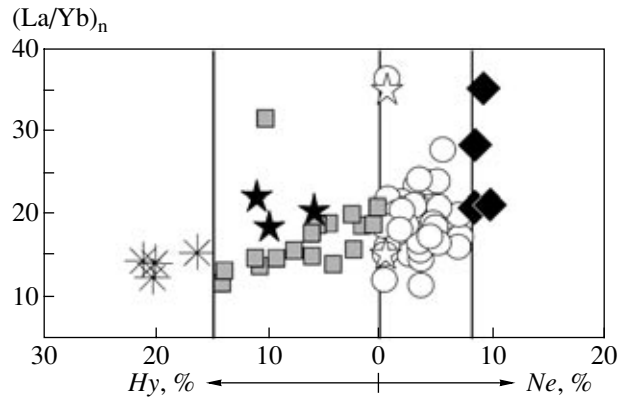


Fig. 5. Variations in the chondrite-normalized (McDonough and Sun, 1995) $(La/Yb)_n$ ratio depending on the silica undersaturation of rocks from the Khubsugul area. No REE were determined in sample MN-266 with 18% normative nepheline. See Fig. 2 for symbol explanations.

very insignificant amount of olivine tholeiites. The $(La/Yb)_n$ ratio increases from the basaltic andesites and olivine tholeiites to hawaiites and basanites (Fig. 5). The essexites fall within the range of the $(La/Yb)_n$ ratio typical of the olivine tholeiites and hawaiites.

CAUSES OF THE CHEMICAL VARIABILITY OF THE LAVAS

Role of Crystallization Differentiation

Figure 6 shows variations in the contents of major oxides and the calculated trends for the crystallization differentiation of olivine, clinopyroxene, and titanomagnetite. The role of plagioclase in the fractionation processes was ignored because of the absence of geochemical indications of this process, such as a relative decrease in the Eu concentration in the chondrite-normalized trace-element patterns and a decrease in the Sr concentration in trace-element patterns normalized to the undifferentiated mantle. The least differentiated compositions for each rock group from the western and eastern walls and from the northern part of the trough were assumed to be low-silica compositions with $Mg\# = 100 \times Mg/(Mg + Fe^{2+})$, atomic quantities, at $Fe^{2+} = 0.85Fe$ within the range of 64.2–68.7% and $MgO > 8$ wt %. The differentiation lines were calculated at a constant composition of the fractionated minerals. Olivine (40 wt % SiO_2 , 7.5 wt % FeO , and 52.5 wt % MgO) and clinopyroxene (48.78 wt % SiO_2 , 1.71 wt % TiO_2 , 10.11 wt % Al_2O_3 , 7.05 wt % FeO , 15.01 wt % MgO) correspond to minerals that crystallized in equilibrium with alkaline basaltic magma in experiments at a pressure of 12.5 kbar (Esin, 1993). Titanomagnetite (14.5 wt % TiO_2 , 5.0 wt % Al_2O_3 , 58.0 wt % FeO , 20.0 wt % Fe_2O_3 , 2.5 wt % MgO) was compositionally close to the average composition of titanomagnetite megacrysts in alkaline basalts from the Baikal rift system (Rasskazov and Ivanov, 1998).

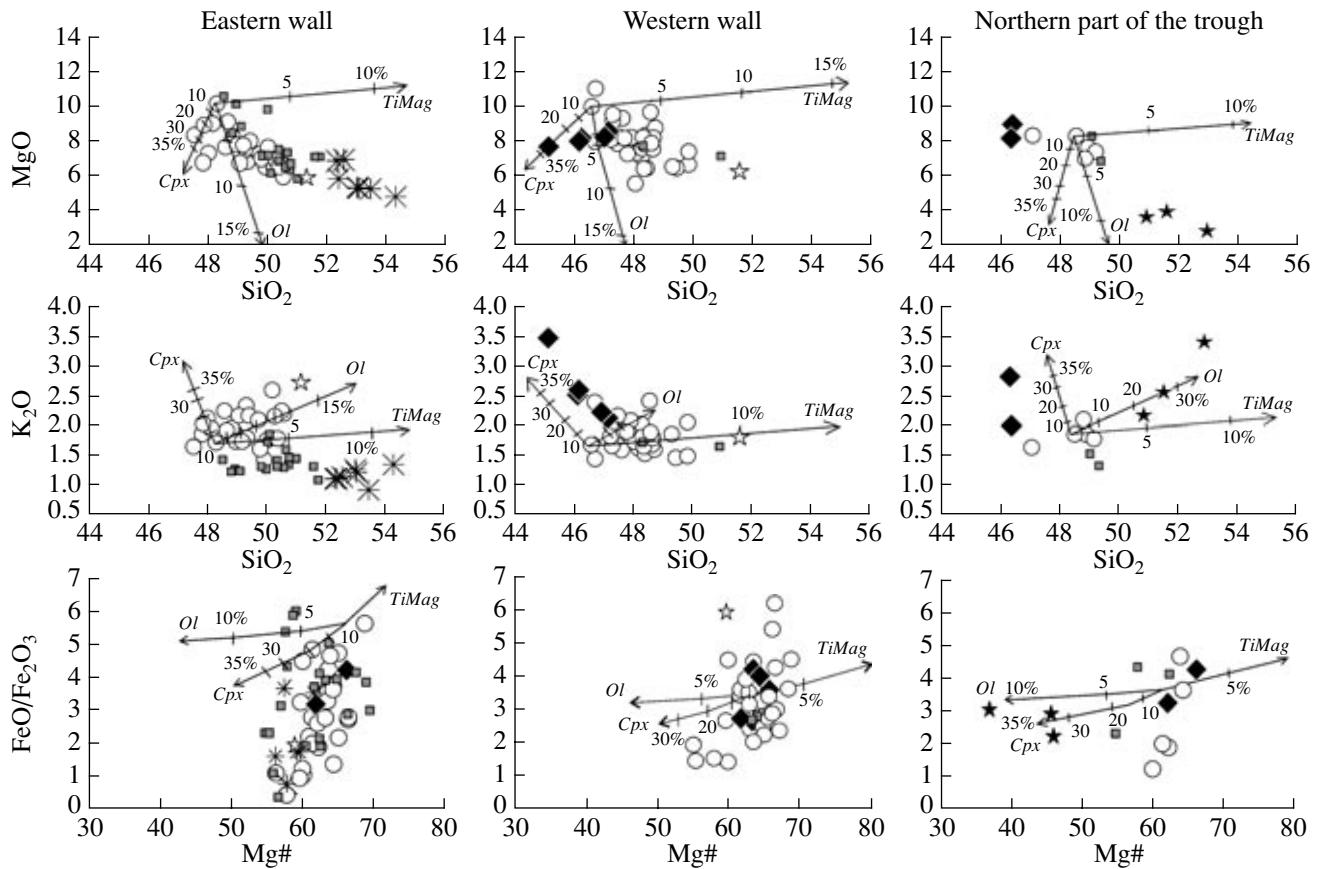


Fig. 6. Variations in the concentrations (wt %) of major components depending on the SiO_2 concentration and the $\text{FeO}/\text{Fe}_2\text{O}_3$ ratio depending on the values of $\text{Mg}\#$ for volcanic rocks from the Khubsugul area.

Arrows show the trends of mineral fractionation in basaltic magma. Minerals: *Ol*—olivine, *Cpx*—clinopyroxene, *TiMag*—titanomagnetite. See Fig. 2 for symbol explanations.

The compositional trends of the Khubsugul basalts cannot be explained by the crystallization differentiation of olivine, clinopyroxene, and titanomagnetite from a single parental melt. For example, the compositional variations are compatible mostly with the simultaneous fractionation of olivine and titanomagnetite in a MgO – SiO_2 diagram, whereas the K_2O – SiO_2 and $\text{FeO}/\text{Fe}_2\text{O}_3$ – $\text{Mg}\#$ diagrams display the opposite trends (Fig. 6). It should be mentioned that most of the analyzed compositions with $\text{Mg}\# < 65\%$ are not primary partial melts derived from magnesian peridotite mantle material. They seem to be derivatives of their own parental melts. The most differentiated essexites occur as lenses in the transitional zone. Their genesis could be related mostly to the fractionation of olivine (10–30%) from a parental hawaiite magma.

Role of Crustal Contamination

Compared to the mantle, the crust is enriched in Th, U, K, Rb, and other incompatible elements (Rudnik and Fountain, 1995). These elements and their ratios serve as indicators of crustal contamination. The Ce/Pb – Nb/U , Ba/Nb – Th/La , and K/Nb – K/Th diagrams

(Fig. 7) show mixing lines for the compositions of OIB and the typical material of the lower, middle, and upper crust. An admixture of lower crustal material (up to 35% and sometimes even as much as 50%) in a basaltic magma does not result in any significant deviations in the concentrations of trace elements from those in the supposed primary partial melts. The contamination of magmas of the OIB type with the material of the upper and middle crust (no more than 20%) leads to insignificant variations in the trace-element ratios at the level of their values in mantle partial melts.

Considering the distribution of the petrographic types of the Khubsugul volcanic rocks relative to the simulated contamination trends, it can be concluded that the variations in the Ce/Pb , Nb/U , Ba/Nb , Th/La , K/Nb , and K/Th ratios are independent of the rock types and mostly cannot be explained by the mixing trends of primary mantle partial melts with various crustal compositions. Hence, even if the parental magmas could be crustally contaminated, this processes did not significantly affect the composition of the basaltic rocks of the Khubsugul area.

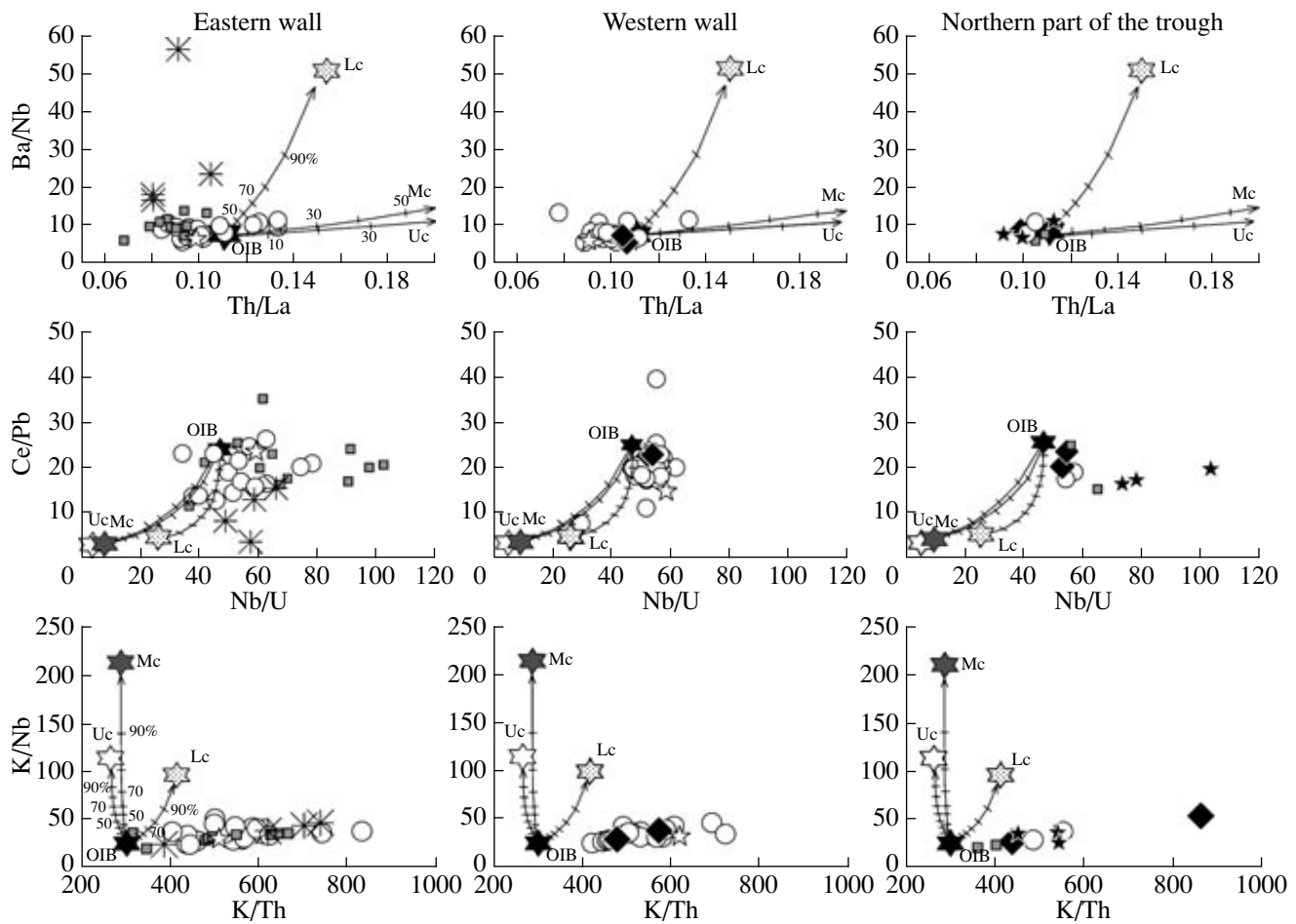


Fig. 7. Variations in trace-element ratios during crustal contamination.

Crust compositions are given after (Rudnick and Fountain, 1995), OIB is after (Sun and McDonough, 1989). Lines show the mixing of OIB with the compositions of lower crust (Lc), middle crust (Mc), and upper crust (Uc). Ticks on the mixing lines are spaced 10% apart. See Fig. 2 for symbol explanations.

Variations in the Degree of Partial Melting of the Mantle

The composition of the parental magmas depends on the degree of the partial melting of the mantle source. To quantify the role of this effect, we simulated the process of equilibrium partial melting (Fig. 8). The assumed model sources were the compositions of garnet and spinel lherzolites. The La and Yb concentrations in the spinel lherzolite were assumed at the levels typical of the primitive mantle (Sun and McDonough, 1989), and the analogous values for the garnet lherzolite were taken up to be 1.2 times higher. We used the following coefficients: $D_{La} = 0.0006$ and $D_{Yb} = 0.0045$ for spinel, $D_{La} = 0.0007$ and $D_{Yb} = 6.4$ for garnet; $D_{La} = 0.0002$ and $D_{Yb} = 0.024$ for olivine; $D_{La} = 0.054$ and $D_{Yb} = 0.43$ for clinopyroxene, and $D_{La} = 0.003$ and $D_{Yb} = 0.032$ for orthopyroxene (Halliday et al., 1995; Hart et al., 1993; Kennedy et al., 1993; Kelemen et al., 1990, 1993). The $(La/Yb)_n$ - Yb_n diagram also exhibits the fractionation lines of olivine and pyroxene, which were calculated by the equation from (Shaw, 1970).

Because of the uncertainties in the selection of the melt sources, $(La/Yb)_n$ - Yb_n diagram allows only qualitative estimation of the degree of partial melting. At an unchanging mineralogy of the source but higher La and Yb concentrations, the calculated degrees of partial melting can increase and, conversely, decrease at lower concentrations.

As follows from the $(La/Yb)_n$ - Yb_n diagram at the chosen parameters, the volcanic rocks of the Khubsugul area were derived from garnet lherzolite at 0.5–5% partial melting. The basaltic andesites and olivine tholeiites are characterized by higher degrees of melting, whereas the basanites and hawaiites show lower degrees, with significant overlaps of the partial melting zones. The shift of the points toward higher Yb_n concentrations at virtually constant $(La/Yb)_n$ ratios can be explained by the equilibrium crystallization of olivine and pyroxene and/or by the addition of spinel lherzolite to the partial melts. The mixing trend between the partial melts derived from garnet and spinel lherzolite is

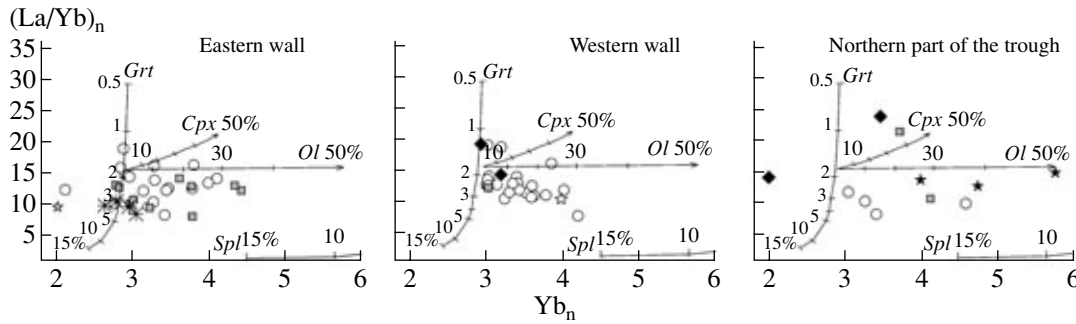


Fig. 8. Variations in the $(La/Yb)_n$ ratio and the Yb_n concentration normalized to the undifferentiated mantle (Sun and McDonough, 1989).

Lines correspond to the melting of garnet (*Grt*) and spinel (*Spl*) lherzolites. The diagram shows calculated degrees of partial melting. The initial concentrations of elements in the melting source were assumed at the level of corresponding values in the undifferentiated mantle for spinel lherzolite (Sun and McDonough, 1989) and 1.2 times higher for garnet lherzolite. Mineral proportions of lherzolite: 55% olivine, 25% orthopyroxene, 15% clinopyroxene, and 5% garnet or spinel. Fractionation lines are calculated by the equation for equilibrium crystallization (Shaw, 1970). The diagram also shows lines for the fractionation of olivine (*Ol*) and clinopyroxene (*Cpx*). Ticks on the mixing lines are spaced 10% apart. See Fig. 2 for symbol explanations.

most clearly pronounced for lavas from the western wall of the Khubsugul trough.

Variations in the Depths at Which the Parental Basaltic Melts Were Derived

Proceeding from experimental data on peridotite melting, Albarede (Albarede, 1992) derived an equation relating the pressure, temperature, and SiO_2 and MgO concentrations in the partial melt

$$P(\text{kbar}) = \exp(0.00252T(^{\circ}\text{C}) - 0.12SiO_2(\text{wt } \%) + 5.027). \quad (1)$$

Later, Hirose and Kushiro (Hirose and Kushiro, 1993) used a method that involved the introduction of diamond powder layer into the experimental ampoule to separate the melt from the source material, which consisted of natural lherzolites HK-66 and KLB-1. The results of these melting experiments were used to evaluate the depths of the derivation of oceanic (Scarrov and Cox, 1995) and continental (Ivanov et al., 1998; Furman, 1995) basalts. In the former of these papers, a simple equation was proposed to relate the SiO_2 concentration in partial melts derived from lherzolite HK-66 and pressure

$$P(\text{kbar}) = 213.6 - 4.05SiO_2(\text{wt } \%). \quad (2)$$

Equations (1) and (2) are applicable only to undifferentiated compositions, because the crystallization differentiation of minerals results in a significant increase in the SiO_2 concentration (Fig. 6). We used another equation to evaluate the pressure:

$$P(\text{kbar}) = 107.9 - 2.19(SiO_2(\text{wt } \%) - 0.85FeO_t(\text{wt } \%)). \quad (3)$$

This equation also makes use of the dependence of the SiO_2 and FeO concentrations in partial melt on pres-

sure (Scarrov and Cox, 1995) but was derived from a more extensive set of experimental data (Hirose and Kushiro, 1993; Falloon et al., 1999) (Fig. 9). The average error of pressure estimates by this equation due to the heterogeneity of the melting lherzolite is ± 2.6 kbar. An increase in the orthopyroxene fraction in the melting source material results in the underestimation of the pressure values at the same SiO_2 and FeO concentrations.

No final derivatives (mugearites and essexites) were used to estimate the pressure, and the compositions of other rocks were recalculated to the hypothetical compositions of parental melts by means of adding olivine of constant composition (Fo_{88}) to the composition of the rock, with an increase in the $Mg\#$ to 72%. Although this procedure is not rigorous, this little affects the pressure estimates by Eq. (3).

Pressure values calculated by Eqs. (1) and (2) (Fig. 10) notably depend on the amount of added olivine. Conversely, the values calculated by Eq. (3) are practically independent of the added olivine amount, which is accounted for by the fact that Eq. (3) includes both the SiO_2 and FeO concentrations, which have the opposite signs. The contents of the two oxides increase in the course of crystallization differentiation, and the difference of these components remains practically unchanging. Because of this, clinopyroxene fractionation also does not affect pressure estimates by Eq. (3).

The scatter of the pressure values calculated by Eq. (3) ranges from 8 to 30 kbar for lavas from the eastern wall of the Khubsugul rift and from 16 to 32 kbar for lavas from its western wall (Fig. 11). In both areas, the distribution of the calculated pressure values is close to Gaussian, a fact indicating that the extreme values are caused by random errors [random analytical errors involved in the lava compositions, errors of the regression line for Eq. (3) due to the variability of the lherzolite composition in the experiments, etc.]. The

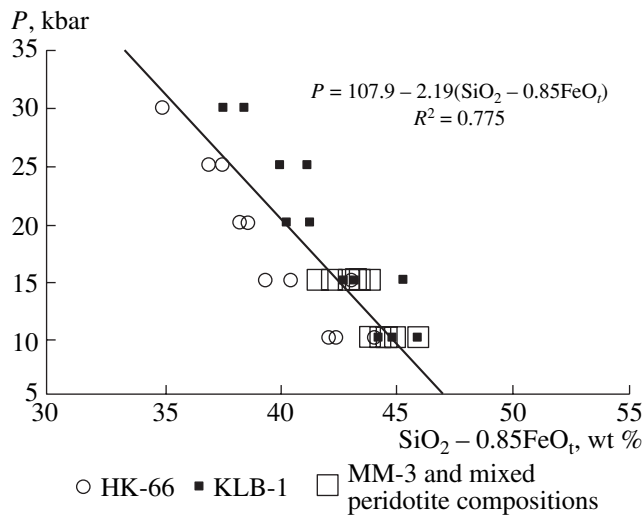


Fig. 9. Dependence of the parameter $\text{SiO}_2 - 0.85\text{FeO}_t$ (wt %) on pressure in experiments on the partial melting of lherzolites HK-66, KLB-1, and MM-3 and synthetic mixed compositions.

Experimental data were compiled from (Hirose and Kushiro, 1993; Falloon et al., 1999). The diagram also shows the line and regression equation for the calculation of pressure (P) and the linear correlation coefficient (R^2).

pressures were evaluated using average values with a dispersion of one standard deviation. For the basalts from the eastern and western walls of the Khubsugul trough, these values are 20.1 ± 3.8 and 24.6 ± 3.2 kbar, respectively, and correspond to depths of 60 ± 12 and 75 ± 10 km, respectively (under the assumption of lithostatic pressure at a crust density of 2.9 g/cm^3 , a mantle density of 3.3 g/cm^3 , and a thickness of the crust of 45 km).

The calculated pressure (and, correspondingly, depth) values significantly overlap. The assumption that the mantle beneath the eastern wall is enriched in orthopyroxene, and the mantle beneath the western wall is, conversely, depleted in this mineral (but rich in olivine), results in practically identical pressure estimates.

The pressures calculated for lavas from the northern part of the trough vary from 16 to 30 kbar, averaging 23.7 kbar (72 km). The limited number of our samples from the transition zone lead to statistical inaccuracies of the estimates, and thus, we did not evaluate the standard deviations.

DISCUSSION AND CONCLUSIONS

Late Cenozoic lavas from the western wall of the Khubsugul rift trough compositionally differ from lavas from the eastern wall. The western wall typically contains hawaiites and subordinate amounts of basanites with occasional compositions of olivine tholeiites, whereas the eastern wall is dominated by hawaiites, olivine tholeiites, and basaltic andesites.

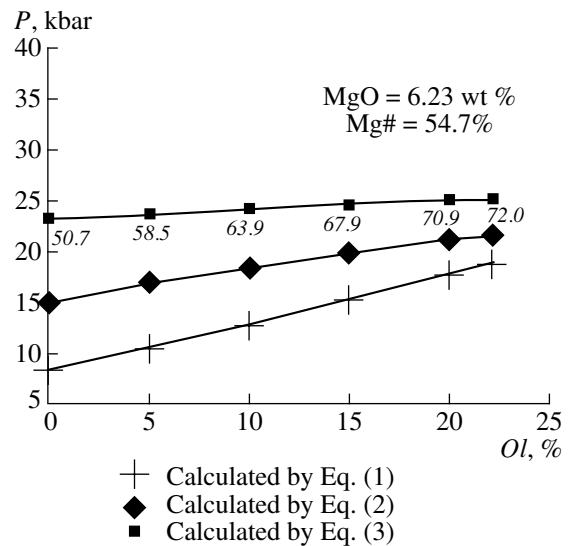


Fig. 10. Diagram for the variations in the calculated pressure (P) values depending on the percentage of olivine needed to add to one of the most differentiated compositions of olivine tholeiites (sample 133) with the lowest $\text{Mg}\#$ value (51.9%) to obtain the parental magma. Numerals correspond to $\text{Mg}\#$ values for hypothetical melts at varying amounts of added olivine.

The differences between the major-component compositions of these rocks were not caused by the processes of crystallization differentiation or crustal assimilation. The effect of the differentiation processes is clearly pronounced only in the development of essexite lenses in a heterogeneous olivine tholeiite flow, as also follows from the model calculations of fractionation trajectories for olivine and, to a lesser extent, pyroxene and titanomagnetite. Essexites were found only in the northern part of the trough. The results of our simulations of the fractionation processes indicate that the essexites could have been produced by the fractionation of a few dozen percent olivine from the parental hawaiite magma (Figs. 6, 7). The genesis of the essexites was most probably related to the unusual condition of the magmatic differentiation. The magmatic melts could be retained in the crust beneath overthrust planes (Rasskazov, 1993).

Yarmolyuk et al. (2003) arrived at the conclusion that “basaltic melts at lower crustal levels can interact with an $\text{H}_2\text{O}-\text{CO}_2$ fluid or be contaminated with recycled lithospheric material enriched in the heavy oxygen isotope” in the southern part of the Baikal rift system. The mixing lines for crustal material and OIB rocks (Fig. 7) suggest the possible effect of crustal contamination. However, these processes alone cannot explain the compositional variability of the volcanic rocks.

Conceivably, the processes of magma generation in the Khubsugul area were controlled by variations in either the melting depths or the composition of the mantle source material. The results of our trace-element simulations of partial melting indicate that the

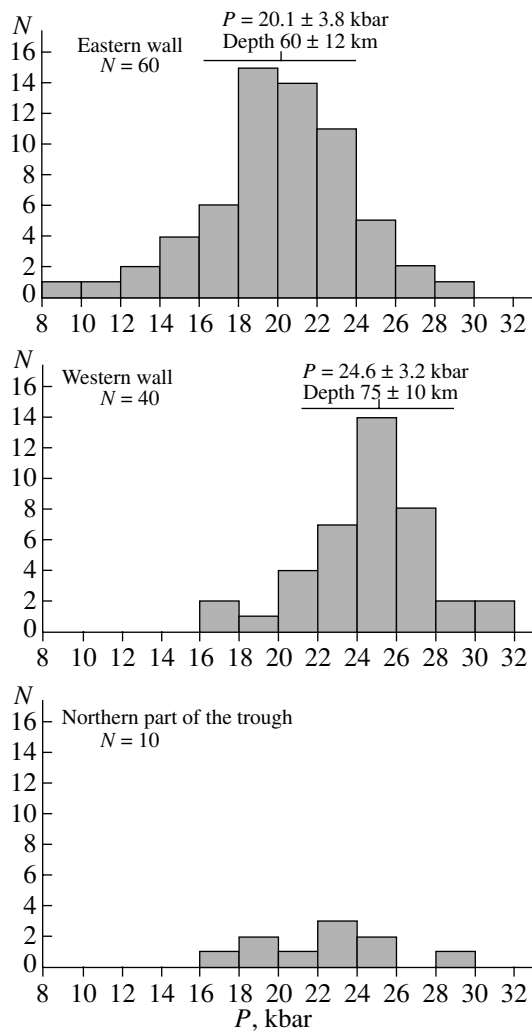


Fig. 11. Histograms for the distribution of pressure (P) calculated for the parental melts of rocks from the western and eastern wall of the Khubsugul trough and the transitional zone.

The diagram shows average pressure and depth values with standard deviations.

basaltic magmas were formed at low degrees of partial melting (0.5–5%) of garnet lherzolite. The basaltic andesites, which were found exclusively in the eastern wall of the Khubsugul trough, are characterized by low degrees of partial melting (3–5%) of garnet lherzolite. We cannot rule out the possibility that the composition of the primary partial melts derived from the garnet lherzolite could be modified in the course of the subsequent fractionation of olivine and/or mixing with partial melts derived from spinel lherzolite. No statistically significant variations in the trace-element compositions of similar rocks were detected across the junction zone of lithospheric blocks of various ages, which suggests that the melted mantle beneath both walls of the Khubsugul trough had a relatively homogeneous composition. The petrochemical variations of the rocks cannot be explained only by the variations in the degree of par-

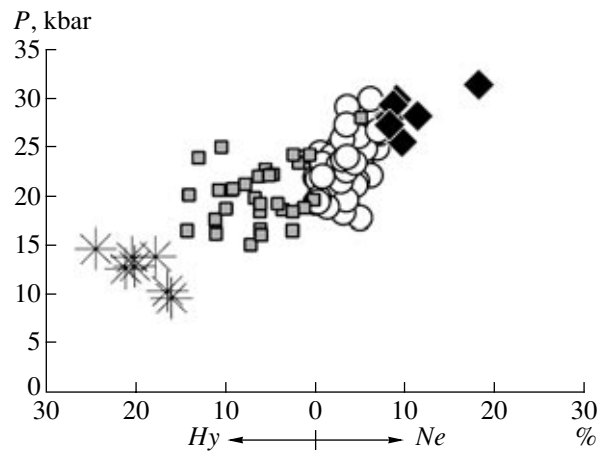


Fig. 12. Correlation between the calculated pressure (P) and degree of silica undersaturation ($Hy-Ne$) for rocks from the Khubsugul area.

See Fig. 2 for symbol explanations.

tial melting of the mantle source. Because of this we suggest that the main factor that controlled the compositional variations of the lavas was variations in the depths at which the melt separated from the melted source due to variations in the lithospheric thickness at the boundaries of the Tuva–Mongolian Massif. Our simulations indicate that the deepest partial melts are the basanites, which were derived under pressures of 25–32 kbar (28 kbar on average, which corresponds to a depth of 86 km) (Fig. 12). The hawaiite partial melts were formed under pressures of 18–30 kbar (23 kbar on average, i.e., at a depth of 70 km), and the olivine tholeiitic melts were derived at 18–30 kbar (20 kbar on average, i.e., at a depth of 60 km). The pressure calculated for the basaltic andesite is equal to 10–15 kbar (13 kbar on average, a depth of 37 km), which corresponds to the range of crustal depths. This makes it possible to regard the basaltic andesites as an unusual rock type, whose composition was likely formed due to the involvement of a less magnesian mantle source material in the melting processes, perhaps, at an increase in the degree of partial melting.

The depth at which basaltic magmas were derived beneath the Tuva–Mongolian Massif averaged 75 ± 10 km (24.6 ± 3.2 kbar) and was equal to 60 ± 12 km (20.1 ± 3.8 kbar) for the Early Caledonian terranes (Fig. 13).

The relative increase in the lava volumes in the eastern wall of the Khubsugul trough compared to that in the western wall likely reflects an increase in the intensity of magmatic processes with decreasing depths at which the magmas were generated with the transition from the thicker lithosphere of the Tuva–Mongolian Massif to the thinner lithosphere of the Early Caledonian terranes.

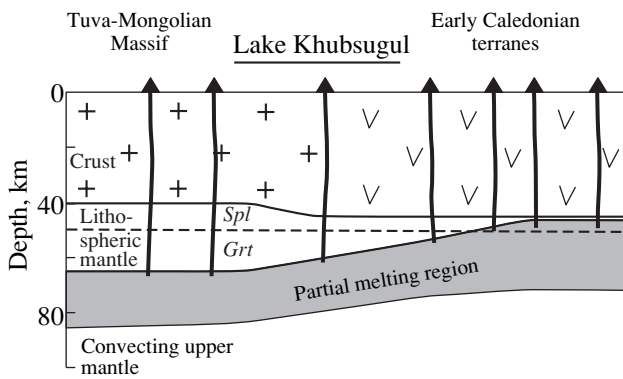


Fig. 13. Schematic representation of the development of Late Cenozoic magmas in the convecting (asthenospheric) mantle beneath lithospheric blocks of various ages.

ACKNOWLEDGMENTS

The authors thank G.V. Bondareva and M.A. Sma-gunova (Institute of the Earth's Crust, Siberian Division, Russian Academy of Sciences) for the determination of major-element concentrations and A.P. Chebykin and E.P. Chebykin (Institute of Limnology, Siberian Division, Russian Academy of Sciences) for help in analytical operations on a PlasmaQuad II+ mass spectrometer. A.B. Perepelov (Vinogradov Institute of Geochemistry, Siberian Division, Russian Academy of Sciences), L.Z. Reznitskii (Institute of the Earth's Crust, Siberian Division, Russian Academy of Sciences), and V.V. Yarmolyuk (Institute of the Geology of Ore Deposits, Petrography, Mineralogy, and Geochemistry, Russian Academy of Sciences) are thanked for constructive criticism during the preparation of the manuscript. This research was conducted within the framework of the Khubsugul Integration Project of the Siberian Division, Russian Academy of Sciences, project 62/2003, and was also financially supported by the Russian Foundation for Basic Research, project no. 05-05-64447, Baikal-RFFI 05-05-97254-r, and Grant MK-1588.2006.5 from the President of the Russian Federation.

REFERENCES

1. F. Albarede, "How Deep do Common Basaltic Magmas Form and Differentiate?" *J. Geophys. Res.* **97** (B7), 10997–11009 (1992).
2. Kh. I. Amirkhanov, A. S. Batyrmurzaev, I. O. Gargatsev, et al., "Age of the Volcanic Basalts of the Udokan Basin (BRZ) and Lake Khubsugul (Mongolia)," *Dokl. Akad. Nauk SSSR* **285**, 411–413 (1989).
3. V. G. Belichenko, E. V. Sklyarov, N. L. Dobretsov, and O. Tomurtogoo, "Geodynamic Map of the Paleo-Asian Ocean. Eastern Segment," *Geol. Geofiz.* **35** (7–8), 29–40 (1994).
4. V. G. Belichenko, L. Z. Reznitskii, N. K. Geletii, and I. G. Barash, "Tuva–Mongolia Massif: Problem of Microcontinents of the Paleo-Asian Ocean," *Geol. Geofiz.* **44**, 554–565 (2003).

5. E. P. Chebykin, M. A. Grachev, E. L. Gol'dberg, et al., "Experience in Working of a Group of Element ICP-MS Analysis of TsKP *Ultramicroanaliz*, Irkutsk," in *Proceedings of 2nd All-Russia Conference. Centers of Collective Use: State and Future Developments*, St. Petersburg, Russia, 2004 (St. Petersburg, 2004) [in Russian].
6. *Classification of Magmatic (Igneous) Rocks and Glossary of Terms. Recommendations of Subcommittee on Systematics of Igneous rocks of the International Geological Science Union* (Nedra, Moscow, 1997) [in Russian].
7. H. Downes, M. K. Reichow, P. R. D. Mason, A.D. Beard, et al., "Mantle Domains in the Lithosphere beneath the French Massif Central: Trace Element and Isotopic Evidence from Mantle Clinopyroxenes," *Chem. Geol.* **200**, 71–87 (2003).
8. S. V. Esin, *Injection Magmatism in the Upper Mantle: Examination of an Empirical Clinopyroxene Geobarometer* (OIGGiM SO RAN, Novosibirsk, 1993) [in Russian].
9. T. J. Falloon, D. H. Green, V. L. Danyushevsky, and U. H. Faul, "Peridotite Melting at 1.0 and 1.5 GPa: an Experimental Evaluation of Techniques Using Diamond Aggregates and Mineral Mixes for Determination of Near-Solidus Melts," *J. Petrol.* **40**, 1343–1375 (1999).
10. T. Furman, "Melting of Metasomatized Subcontinental Lithosphere: Undersaturated Mafic Lavas from Rungwe, Tanzania," *Contrib. Mineral. Petrol.* **122**, 97–115 (1995).
11. A. N. Halliday, D.-C. Lee, S. Tommasini, G. R. Davies, et al., "Incompatible Trace Elements in OIB and MORB and Source Enrichment in the Sub-Oceanic Mantle, Earth Planet. Sci. Lett." **133**, 379–395 (1995).
12. S. R. Hart and T. Dunn, "Experimental *Cpx/Melt* Partitioning of 24 Trace Elements," *Contrib. Mineral. Petrol.* **113**, 1–8 (1993).
13. K. Hirose and I. Kushiro, "Partial Melting of Dry Peridotites at High Pressure: Determination of Compositions of Melts Segregated from Peridotite Using Aggregates of Diamond," *Earth Planet. Sci. Lett.* **114**, 477–489 (1993).
14. A. V. Il'in, "Tuva–Mongolian Massif," in *Proceedings of Regional Geology of Africa and Foreign Asia* (NII "Zarubezhgeologiya", Moscow, 1971), issue 22, pp. 67–73 [in Russian].
15. V. V. Ivanenko, M. I. Karpenko, R. M. Yashina, et al., "New Data on K–Ar Age of Basalts from the Western Flank of the Khubsugul Rift, Mongolia," *Dokl. Akad. Nauk SSSR* **309**, 925–930 (1989).
16. A. V. Ivanov, S. V. Rasskazov, A. Boven, et al., "Late Cenozoic Alkaline–Ultrabasic and Alkaline Basanite Magmatism of the Rungwe Province, Tanzania," *Petrologiya* **6**, 228–250 (1998) [*Petrology* **6**, 208–229 (1998)].
17. M. J. Le Bas and A. L. Streckeisen, "The IUGS Systematics of Igneous Rocks," *J. Geol. Soc. London* **148**, 825–833 (1991).
18. P. B. Kelemen, K. T. M. Johnson, R. J. Kinzler, and A. J. Irving, "High Field Strength Element Depletions in Arc Basalts due to Mantle–Magma Interaction," *Nature* **345**, 521–524 (1990).
19. P. B. Kelemen, N. Shimizu, and J. T. Dunn, "Relative Depletion of Niobium in Some Arc Magmas and the Continental Crust: Partitioning of K, Nb, La, and Ce dur-

- ing Melt/Rock Reaction in the Upper Mantle,” *Earth Planet. Sci. Lett.* **120**, 111–133 (1993).
20. A. K. Kennedy, G. E. Lofgren, and G. J. Wasserburg, “An Experimental Study of Trace-Element Partitioning between Olivine, Orthopyroxene and Melt in Chondrules—Equilibrium Values and Kinetic Effects, *Earth Planet. Sci. Lett.* **115**, 177–195 (1993).
 21. S. D. King and D. Anderson, “Edge-driven Convection,” *Earth Planet. Sci. Lett.* **160**, 289–296 (1998).
 22. A. I. Kiselev, M. E. Medvedev, and G. A. Golovko, *Volcanism of the Baikal Rift Zone and Problem of Deep Magma Generation* (Nauka, Novosibirsk, 1979) [in Russian].
 23. A. B. Kuz'michev, *Tectonic Evolution of the Tuva–Mongolian Massif: Early Baikalian, Late Baikalian, and Early Caledonian Stages* (PROBEL-2000, Moscow, 2004) [in Russian].
 24. P. T. Leat, R. N. Thompson, M. A. Morrison, G. L. Hendry, et al., “Alkaline Hybrid Mafic Magmas of the Yampa Area, NW Colorado, and Their Relationship to the Yellowstone Mantle Plume and Lithospheric Mantle Domains”, *Contrib. Mineral. Petrol.* **107**, 310–327 (1991).
 25. X. Lenoix, C. J. Carrido, J. L. Bodinier, and J. M. Dautria, “Contrasting Lithospheric Mantle Domains Beneath the Massif Central (France) Revealed by Geochemistry of Peridotite Xenoliths,” *Earth Planet. Sci. Lett.* **181**, 359–375 (2000).
 26. *Magmatic Rocks: Classification, Nomenclature, and Petrography* (Nauka, Moscow, 1985), Vol. 1 [in Russian].
 27. W. F. McDonough and S.-S. Sun, “The Composition of Earth,” *Chem. Geol.* **120**, 223–253 (1995).
 28. M. A. Menzies, “Cratonic, Circumcratonic and Oceanic Mantle Domains beneath the Eastern United States,” *J. Geophys. Res.* **94** (B6), 7899–7915 (1989).
 29. J. S. Miller, A. F. Glazner, G. L. Farmer, I. B. Suayah, and L. A. Keith, “A Sr, Nd, and Pb Isotopic Study of Mantle Domains and Crustal Structure from Miocene Volcanic Rocks in the Mojave Desert, California,” *Geol. Soc. Amer. Bull.* **112**, 1264–1279 (2000).
 30. A. Peccerillo and G. F. Panza, “Upper Mantle Domains beneath Central–Southern Italy: Petrological, Geochemical and Geophysical Constraints,” *Pure Appl. Geophys.* **156**, 421–443 (1999).
 31. S. V. Rasskazov, J. F. Luhr, S. A. Bowring, A. V. Ivanov, et al., “Late Cenozoic Volcanism in the Baikal Rift System: Evidence for Formation of the Baikal and Khubsugul Basins due to Thermal Impacts on the Lithosphere and Collision-Derived Tectonic Stress,” in *Berliner Paläobiologische Abhandlungen (special “Ancient Lakes” issue)*, Ed. by A.V. Ivanov, F. Riedel, O. A. Timoshkin, and G. Coulter (Frei Univeristät Berlin, Berlin, 2003).
 32. S. V. Rasskazov and A. V. Ivanov, “Redox Conditions of Magmatism of Hot Spot and Extensional Zones in the Baikal Rift System,” in *Precambrian Structural–Compositional Complexes of Eastern Siberia* (Irkutsk. Univ., Irkutsk, 1998), pp. 44–58 [in Russian].
 33. S. V. Rasskazov, “Basalts and Structural Evolution of the Western Termination of the Baikal Rift Zone,” *Geokhimiya*, No. 4, 614–619 (1990).
 34. S. V. Rasskazov, *Magmatism of the Baikal Rift System* (Nauka, Novosibirsk, 1993) [in Russian].
 35. S. V. Rasskazov, A. V. Ivanov, and E. I. Demonterova, “Deep Nodules in the Zun–Murina Basanites, Tunkin Rift Valley, Baikal Area,” *Geol. Geofiz.* **40** (1), 100–110 (2000).
 36. S. V. Rasskazov, E. V. Saranina, N. A. Logachev, et al., “The DUPAL Mantle Anomaly of the Tuva–Mongolian Massif and Its Paleogeodynamic Implication,” *Doklady Akad. Nauk* **382**, 110–114 (2002b) [*Dokl. Earth Sci.* **382**, 44–48 (2002b)].
 37. S. V. Rasskazov, S. A. Bowring, T. Hawsh, et al., “The Pb, Nd, and Sr Isotope Systematics in Heterogeneous Continental Lithosphere above the Convecting Mantle Domain,” *Dokl. Akad. Nauk* **387**, 519–523 (2002a) [*Dokl. Earth. Sci.* **387**, 1056–1059 (2002a)].
 38. R. L. Rudnick and D. M. Fountain, “Nature and Composition of the Continental Crust: A Lower Crustal Perspective,” *Rev. Geophys.* **33**, 267–309 (1995).
 39. J. H. Scarrow and K. G. Cox, “Basalts Generated by Decompressive Adiabatic Melting of a Mantle Plume: A Case Study from the Isle of Skye, NW Scotland,” *J. Petrol.* **36**, 3–22 (1995).
 40. D. M. Shaw, “Trace Element Fractionation During Anatexis,” *Geochim. Cosmochim. Acta.* **34**, 237–243 (1970).
 41. S.-S. Sun and W. F. McDonough, “Chemical and Isotopic Systematics of Oceanic Basalts: Implications for Mantle Composition and Processes,” in *Magmatism in the Ocean Basins*, Ed. by A. D. Saunders and M. J. Norry, *Geol. Soc. Spec. Publ.* **42**, 313–345 (1989).
 42. R. N. Thompson and S. A. Gibson, “Subcontinental Mantle Plumes, Hotspots and Pre-Existing Thinspots”, *J. Geol. Soc. London* **148**, 973–977 (1991).
 43. E. P. Vasil'ev, V. G. Belichenko, and L. Z. Reznitskii, “Relationship between Ancient and Cenozoic Structures at the Southwestern Flank of the Baikal Rift Zone,” *Dokl. Akad. Nauk* **353**, 785–792 (1997) [*Dokl. Earth. Sci.* **353**, 381–384 (1997)].
 44. V. V. Yarmolyuk, V. G. Ivanov, V. I. Kovalenko, and B. G. Pokrovskii, “Magmatism and Geodynamics of the Southern Baikal Volcanic Region (Mantle Hot Spot): Results of Geochronological, Geochemical, and Isotopic (Sr, Nd, and O) Investigations,” *Petrologiya* **11**, 3–34 (2003) [*Petrology* **11**, 1–30 (2003)].
 45. T. A. Yasnygina, S. V. Rasskazov, M. E. Markova, et al., “ICP-MS Trace-Element Determination in the Basic–Intermediate Volcanic Rocks Using Microwave Acid Decomposition,” in *Applied Geochemistry. Analytical Investigations*, Ed. by E. K. Burenkov and A. A. Krementetskii (IMGRE, Moscow, 2003) [in Russian].
 46. Yu. A. Zorin, V. G. Belichenko, E. Kh. Turutanov, et al., “Central Siberian–Mongolian Transect,” *Geotektonika*, No. 2, 3–19 (1993).